Electronic Supplementary Material (ESI) for Nanoscale.

In-situ TEM investigation of nucleation and crystallization of hybrid bismuth nanodiamonds

Sihan Ma[a,b], Yipeng Li[a,b], Dewang Cui[a,b], Gang Yang[a,b], Lin Wang[*,c],Guang Ran[*,a,b]

[a] College of Energy, Xiamen University, Xiamen 361002, China

[b] Fujian Provincial Nuclear Energy Engineering Technology Research Center, Xiamen 361002, China

[c] School of Medicine, Xiamen University, Xiamen 361002, China

*Corresponding author：Guang Ran (College of Energy, Xiamen University), Email: gran@xmu.edu.cn ; Lin Wang (School of Medicine, Xiamen University), E-mail: wanglin_linda82@163.com

Supplementary Materials

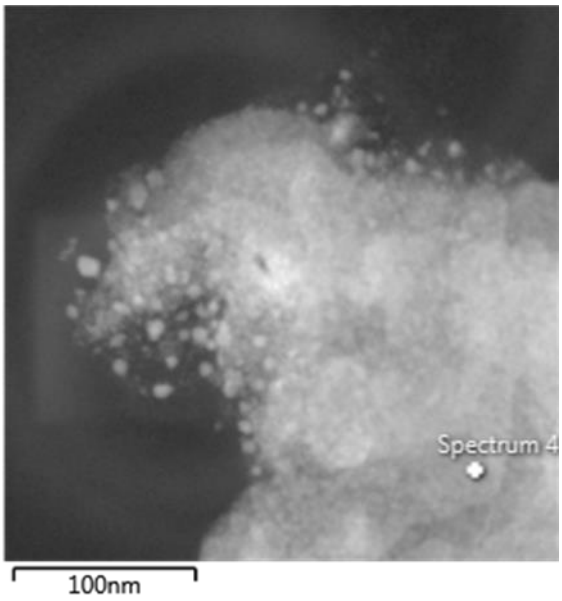

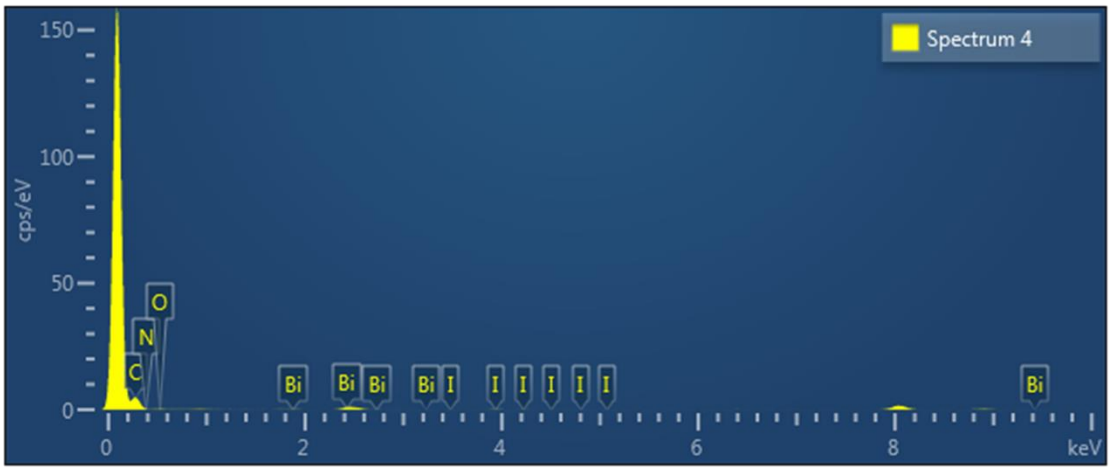

Element	Line Type	k Factor	k Factor type	Absorption Correction	Wt%	Wt% Sigma	Atomic %
C	K series	3.187	Theoretical	1.00	0.00	0.00	0.00
N	K series	1.843	Theoretical	1.00	0.00	0.00	0.00
O	K series	1.480	Theoretical	1.00	2.92	0.77	26.48
I	L series	1.914	Theoretical	1.00	13.68	0.89	15.63
Bi	M series	1.767	Theoretical	1.00	83.40	1.11	57.89
Total:					100.00		100.00

Figure. S1 STEM image and EDS of the BiOI matrix with Bi growth, indicating the composition of the BiOI matrix.

The corresponding point represents the composition of the matrix, mainly including Bi, O, I, C and so on. The elemental content analysis of the interested region is given in this table, suggesting that the matrix is BiOI because of the relative atomic ratio.

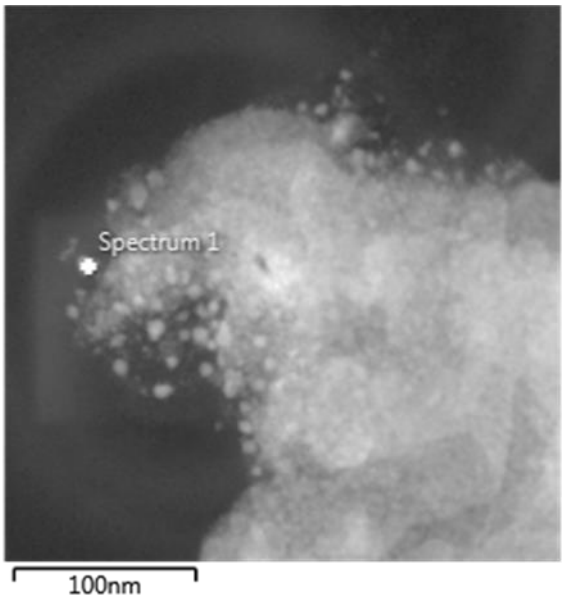

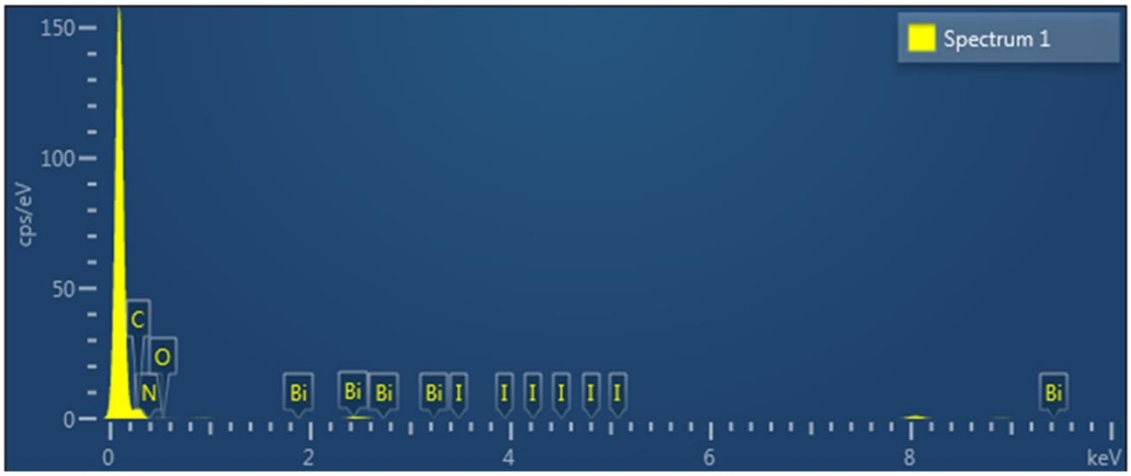

Element	Line Type	k Factor	k Factor type	Absorption Correction	Wt%	Wt% Sigma	Atomic %
C	K series	3.187	Theoretical	1.00	0.00	0.00	0.00
N	K series	1.843	Theoretical	1.00	0.00	0.00	0.00
O	K series	1.480	Theoretical	1.00	0.79	1.10	9.33
I	L series	1.914	Theoretical	1.00	0.77	0.84	1.15
Bi	M series	1.767	Theoretical	1.00	98.45	1.38	89.52
Total:					100.00		100.00

Figure. S2 STEM image and EDS of the BiOI matrix with Bi growth, indicating the emergence of the Bi particles.

Similarly, the corresponding cursor marks the region of interest, and the EDS illustrates the effective elemental distribution. The target particle is rationally verified by using the EDS analysis in this table, suggesting that the target particle is Bi because of 89% atomic ratio.

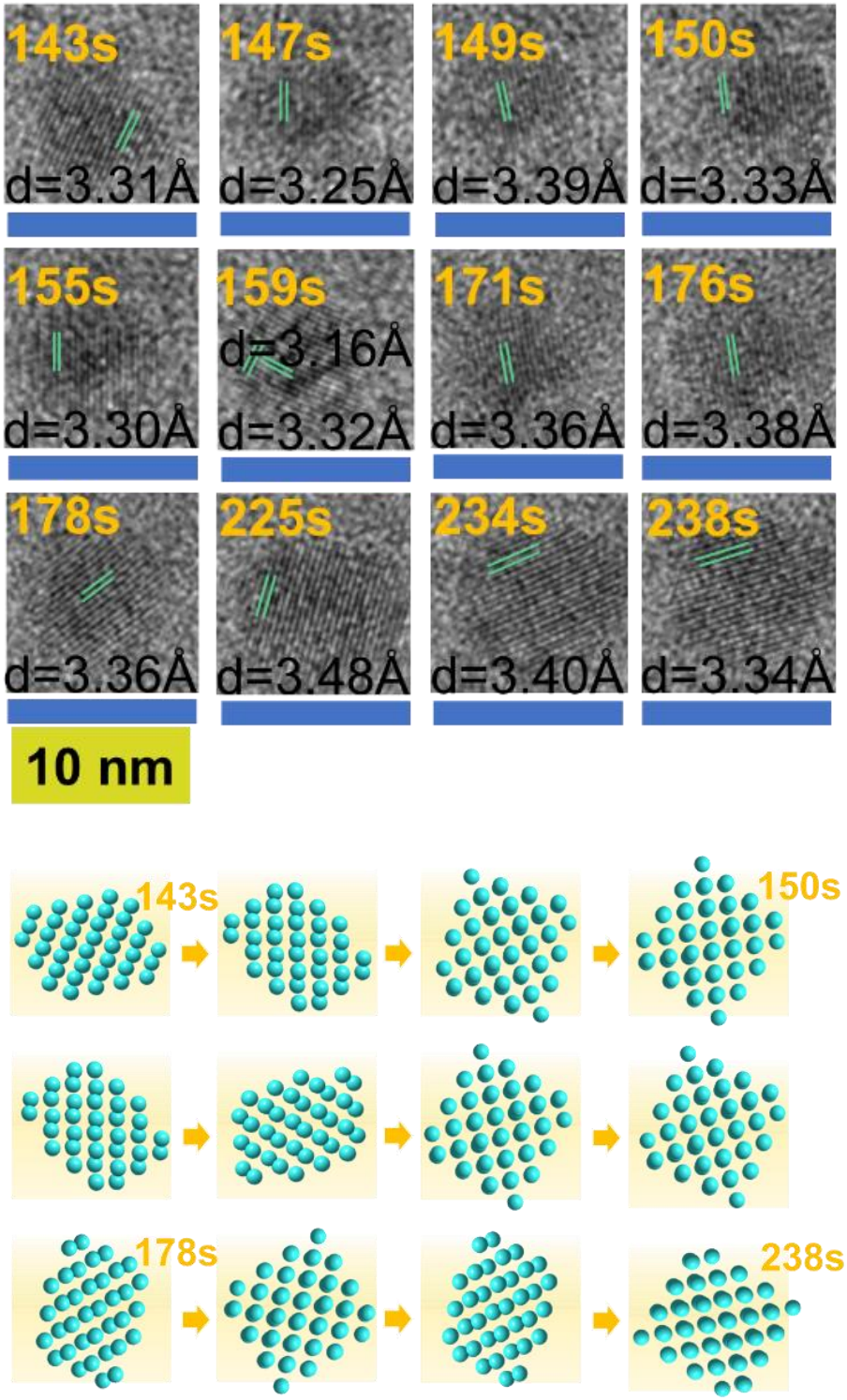

Figure. S3 The facet orientation of Bi nanocrystal at different viewing times. The marked lattice spacing and corresponding given facet orientation models.

With the increase of electron irradiation times, the interesting phenomenon includes fluctuation between amorphous and crystalline, the growth of surface Bi particle verify

the repetition of nucleation and crystallization. In the meantime, results show the different orientations of the electron-induced Bi nanocrystal at the end of amorphous. The measurement lattice spacing is well matched with the (012) plane of element Bi. Conceivably, the disordered Bi atoms can be rearranged and put together, finally form the new nanocrystal. The nanodroplet with liquid nature can cause its own disordered atoms to tumble around at will situation, further the formation of random nanocrystal composition at natural ripening conditions.

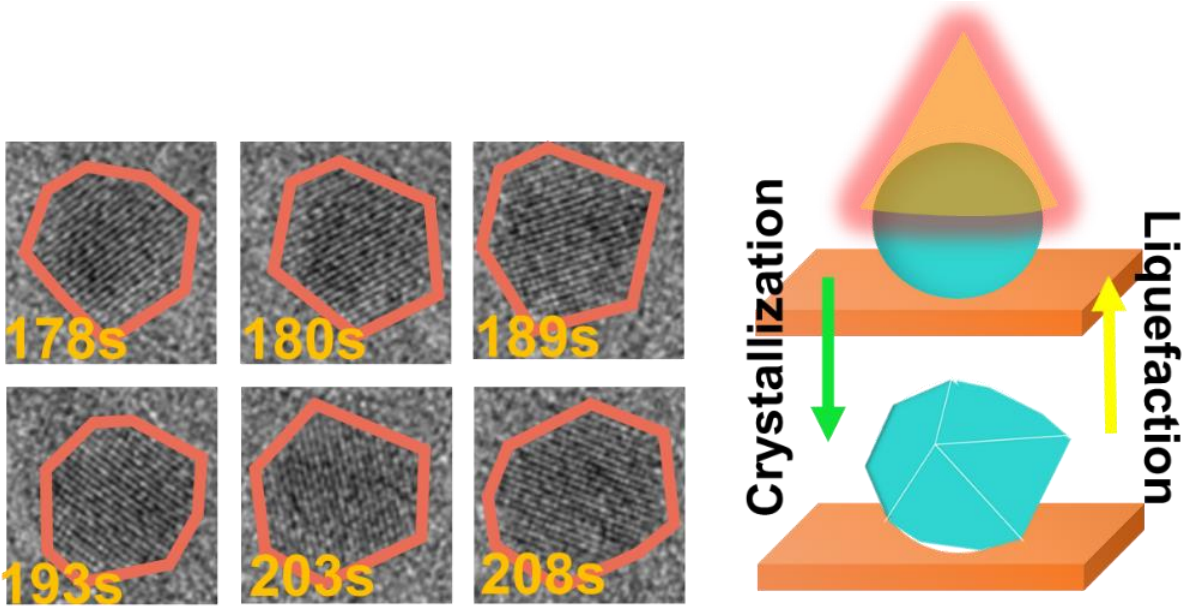

Figure. S4 Morphological observation of Bi nanocrystal at different times. The given droplet and diamond model.

With the passage of electron bombardment time, the nanocrystal presents different section phases, indicating the effective rotation effect in the sustainable recrystallization procedure. Combining with the interface growth graphics (Figure 2c), the possible nanocrystal morphology can be depicted in the corresponding model, implying the existence of nanodiamond with polyhedral structure.

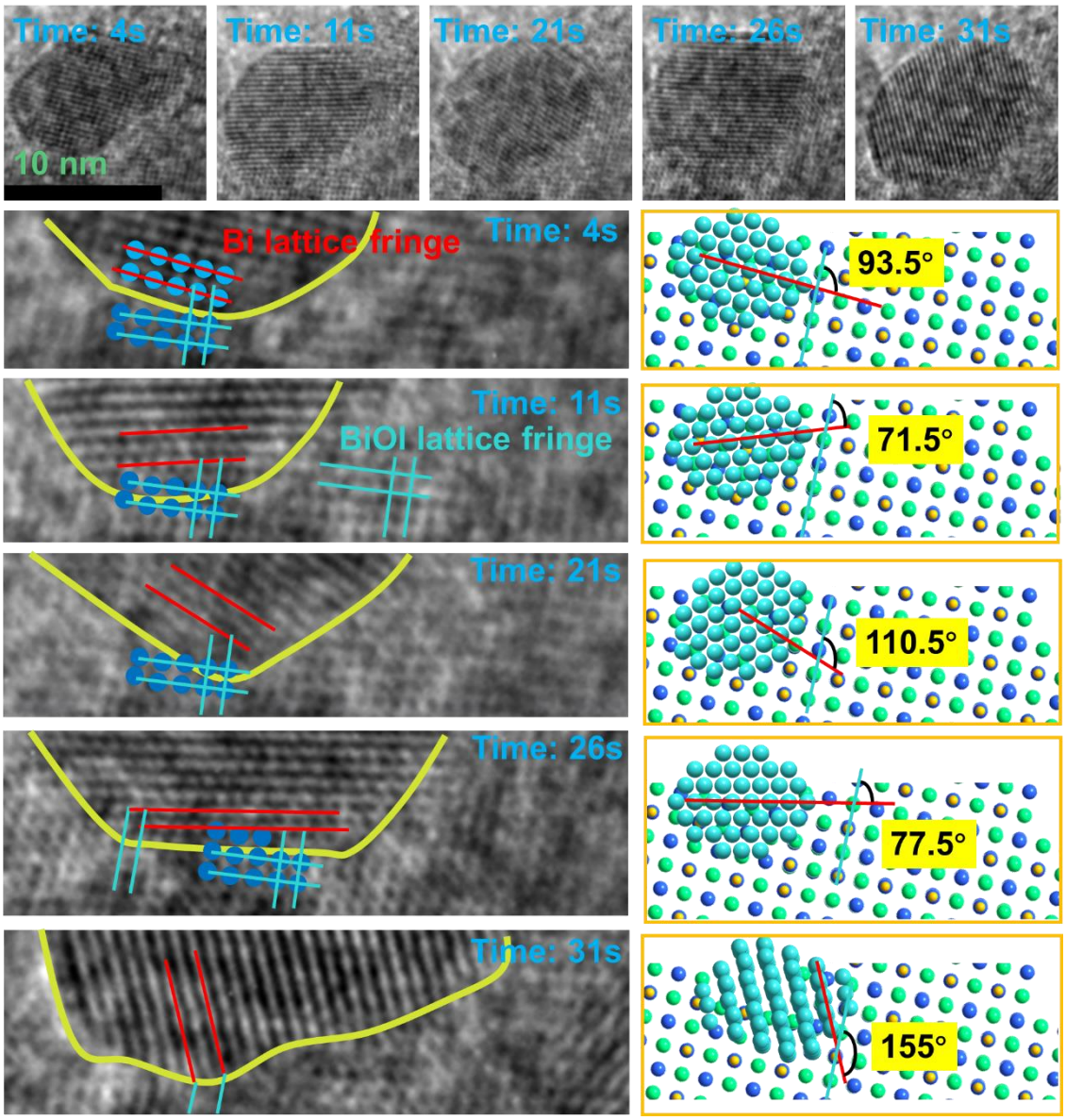

Figure. S5 Interface angle analysis between Bi nanodiamond and BiOI matrix.

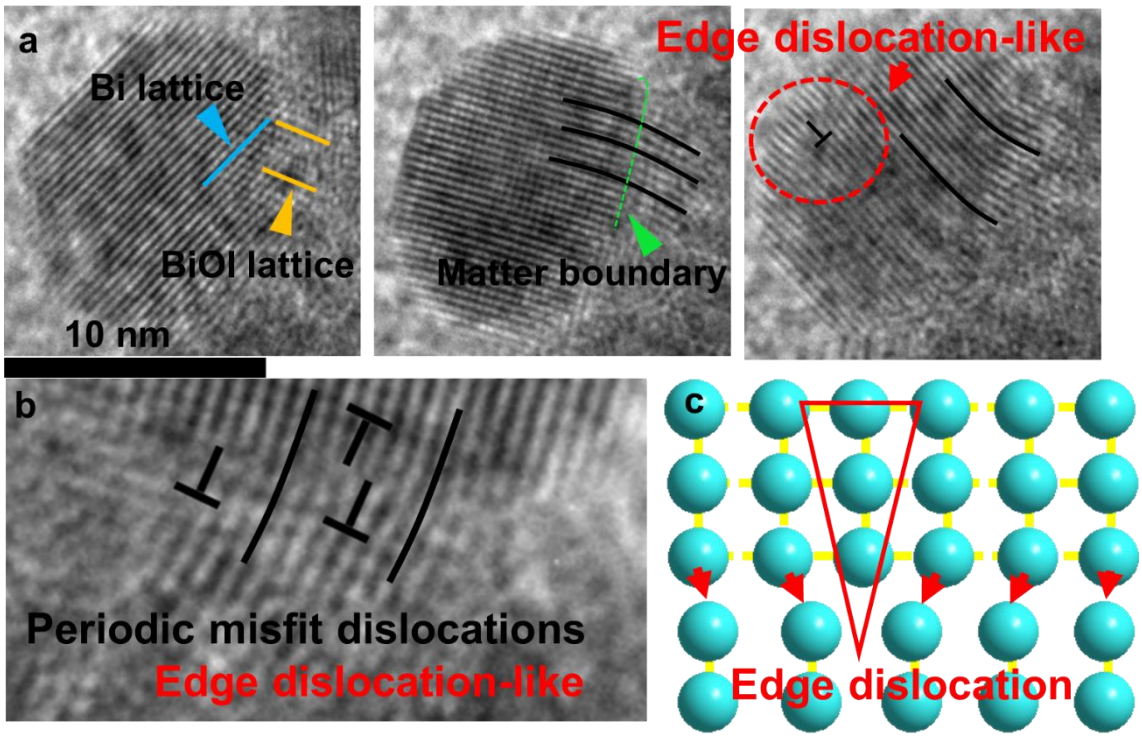

Figure. S6 The behavior of lattice fringes during interface reaction between Bi nanodiamond and BiOI matrix. (a) HRTEM images of Bi nanodiamond on the boundary of BiOI at different imaging times. (b) The selected enlarged region towards the effective observation of interface interaction. (c) The schematic illustration of the edge dislocation.

The interface behavior between the metal catalyst and matrix plays a critical role in heterogeneous catalysis. Their catalytic activity depends on the interface between the nanoparticle and its substrate since the most active site in many reactions is located at the perimeter interface. In heterogeneous crystallization, the interface between Bi and BiOI is observed. In addition to the reversible dynamic evolution between liquid and solid, the solid-solid contacting interface exhibits different atomic distributions. In the process of nucleation and crystallization, the rotation of Bi cluster between nucleation and crystallization process to form nanocrystal that can affect the ordered distribution of atoms owing to the rapidly rotating stresses and interfacial atomic forces. Experimental results show the presence of edge dislocation-like in nanodiamond and interface.

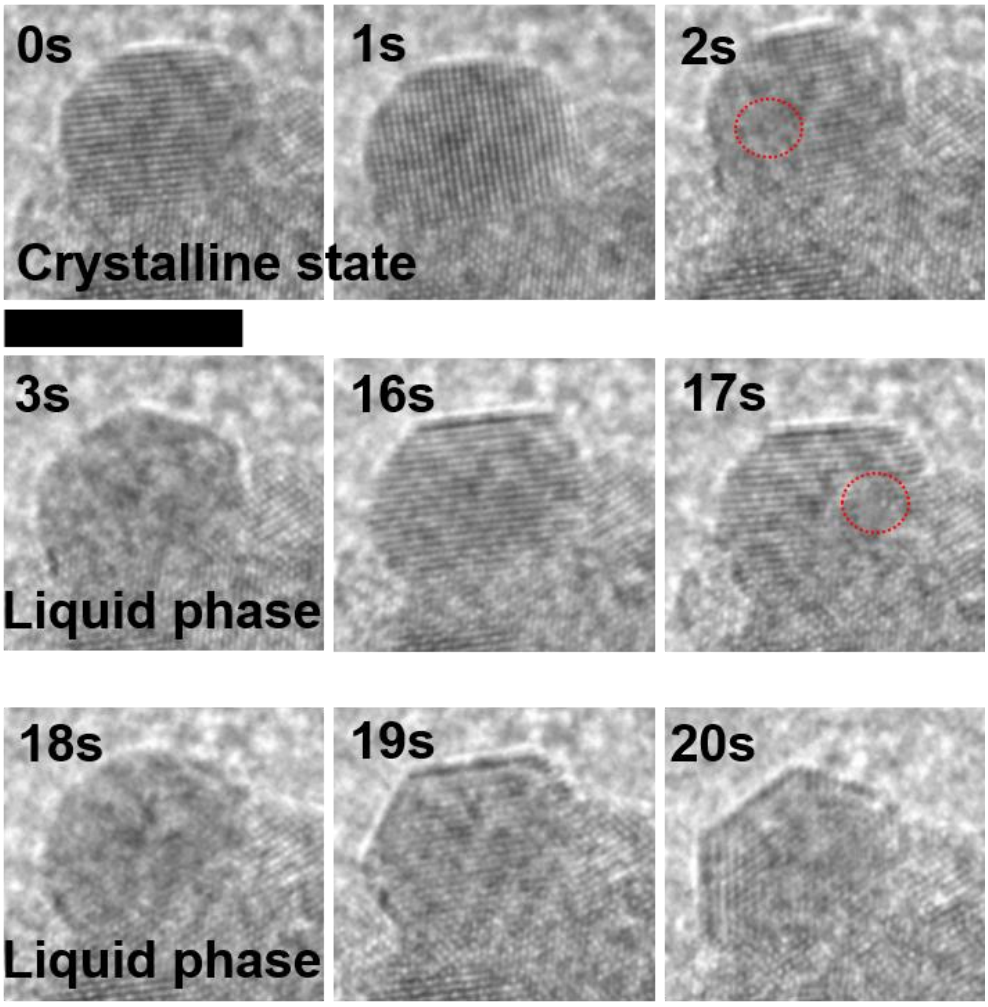

Figure. S7 The fluctuation dynamic process of Bi nanodiamond, including surface melting and diffusion, recrystallization.

The effective melting and freezing mechanism can be observed. Firstly, the local surface melting occurs, and further, the melting zone effectively expands to form the final liquid state.

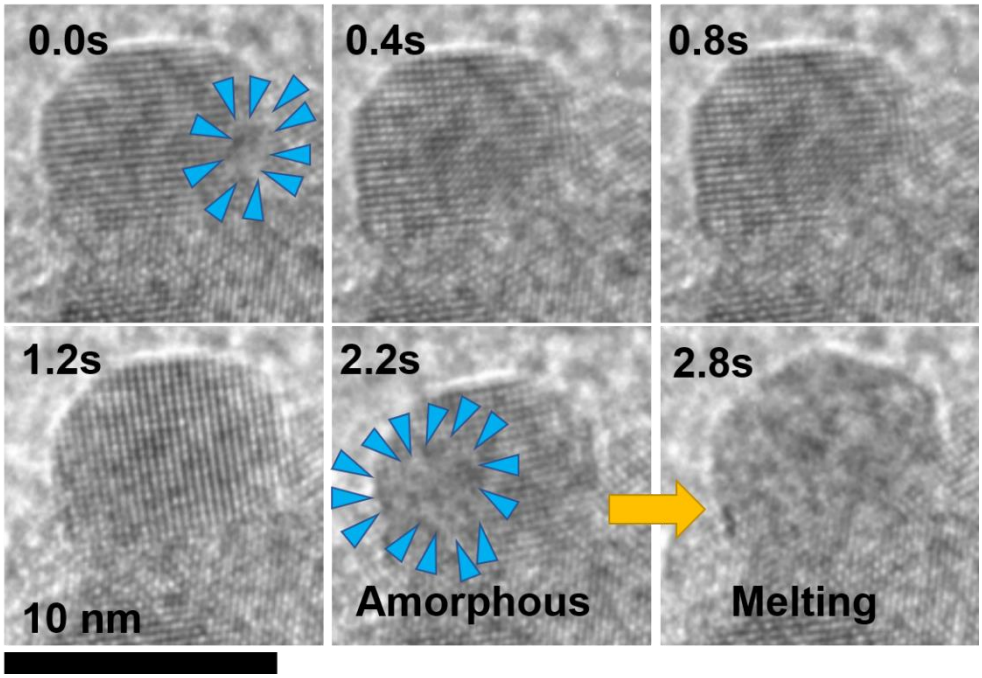

Figure. S8 The HRTEM images with subsecond temporal resolution of Bi nanodiamond formation between 0 and 3s.

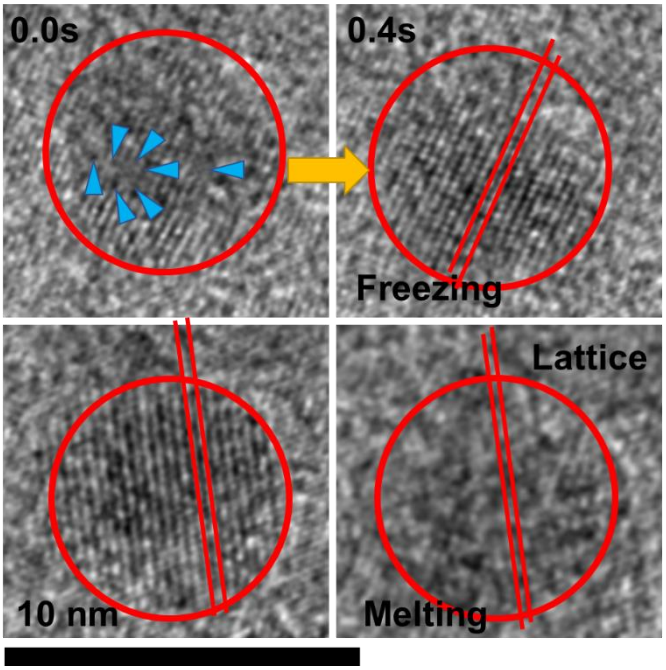

Figure. S9 The lattice state of Bi nanodiamond during the melting and freezing process.

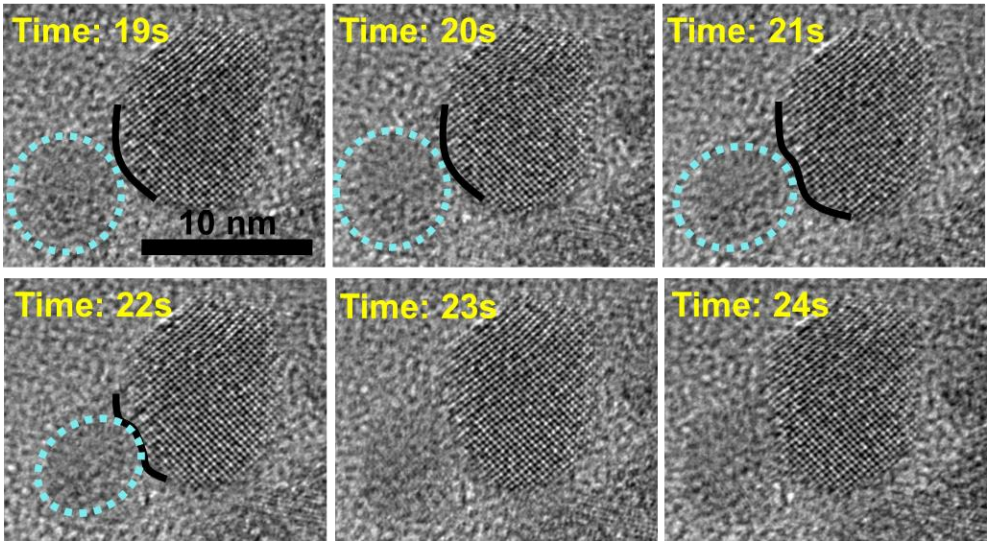

Figure. S10 The available collision dynamics of liquid-solid Bi nanoparticles during the migration procedure.

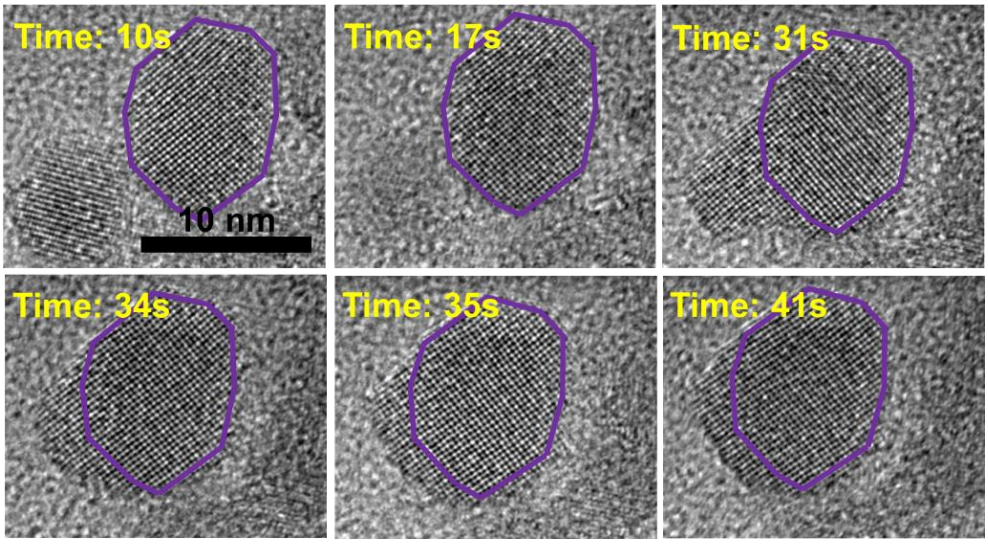

Figure. S11 The fusion region area of Bi nanodiamond after the migration process. The atoms fuse by diffusion along the edge of the Bi particle, and the main object area retains a similar area, an extra Bi particle complements the increased area.

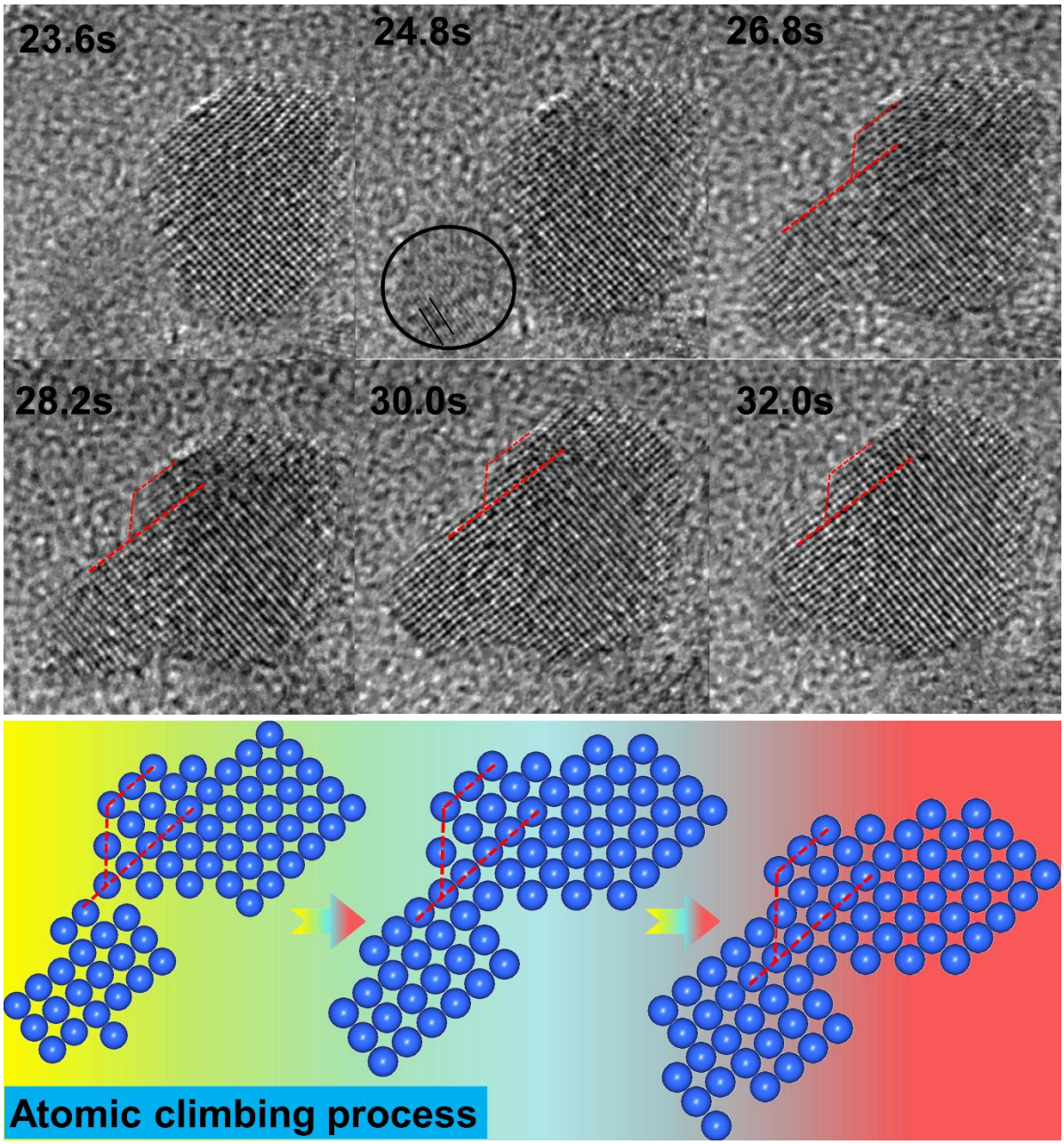

Figure. S12 An effective atomic climbing process during the fusion.

During the Bi particle fusion, the contacting atoms in face-to-face interactions to form crystals, and further providing a motion for surrounding atoms. A small Bi particle was absorbed by a big one, which induced the small Bi particle atoms to approach large particle atoms. Gradually, the small Bi particle atoms climb along the large Bi particle boundary atoms. Atoms overcome the strong forces between metal atoms to achieve effective fusion.

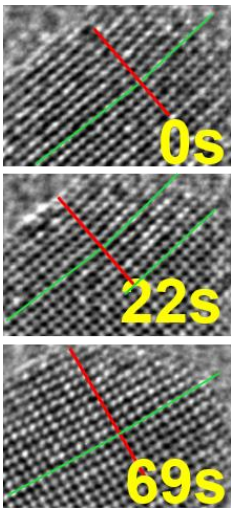

Figure. S13 The co-lattice small angle twin behavior before and after Bi nanoparticle fusion.

Reference:

1. Lin, Z.; Shao, G.; Liu, W.; Wang, Y.; Wang, H.; Wang, H.; Fan, B.; Lu, H.; Xu, H.; Zhang, R., In-situ TEM observations of the structural stability in carbon nanotubes, nanodiamonds and carbon nano-onions under electron irradiation. *Carbon* **2022,** *192*, 356-365.